

Development and performance evaluation of a bricklaying gantry-based parallel robot manipulator

Musa Hassan Ibrahim¹, Umar Ali Umar^{1, *}, Matthew Afolayan Olatunde¹,
Ayodeji Nathaniel Oyedeji¹

¹Department of Mechanical Engineering, Ahmadu Bello University, Zaria, 810107,
Nigeria

*Corresponding Author: Umar Ali Umar. Email: umaraliumar@yahoo.co.uk

Abstract: Gantry robots are still used in wide application areas, especially pick and place applications. However, there is a gap in the utility of these robots in the building sector, particularly for the pick-and-place application of building blocks from and to a predefined location. The Gantry-based robot is considered a parallel manipulator because, unlike serial manipulators, the load is divided among its multiple links/legs or arms; this is just so because it is made up of more than one link. Hence, this research presents a study in the field of linear and nonlinear model fit system identification on the aforementioned robot through an attempt to provide a better design to take care of the limitations of parallel manipulators, small workspace problems and robot mobility problems. In this study, Arduino Mega was used for the control system. Other materials included bipolar nema17 stepper motors, MG996R servo motor, A4988 driver, sprocket and chain, belt, pulley and buggy wheels, while SolidWorks was used for the system's design and simulation. Aluminium (Al alloy 6061) was used for the robot construction due to its excellent properties and suitability. Actuators and parts were analyzed and modelled to gain knowledge of the kinematic behaviour, and the analyses established the linear and nonlinear identification of model fitness. This study used a compact model fit system and a two-method validation identification procedure. The results show that the system model can be successfully identified and validated from the measured data and provide a near-accurate estimate between hypothetical and measured data. Two experimental validations gave 94% using the first setup and 97% using the second setup. This provides a 0.8% progress increment from previous studies.

Keywords: Gantry robot, Robot manipulator, Simulation, Validation, Linear and nonlinear model, Model fit.

التطوير وتقييم الأداء لمناور روبوت متوازي قائم على جسر من الطوب

الملخص: لا تزال الروبوتات العملاقة مستخدمة في مجالات التطبيق الواسعة ، وخاصة تطبيقات الالتقاط والمكان. ومع ذلك ، هناك فجوة في فائدة هذه الروبوتات في قطاع البناء ، لا سيما لتطبيق الانتقاء والمكان لبنات البناء من وإلى موقع محدد مسبقاً. يعتبر الروبوت القائم على جسر الرافعة من المناور المتوازي لأنه ، على عكس المتلاعبين التسلسليين ، يتم تقسيم الحمل بين الوصلات / الأرجل أو الأذرع المتعددة ؛ هذا فقط لأنه يتكون من أكثر من ارتباط واحد. ومن ثم ، يقدم هذا البحث دراسة في مجال تحديد النظام الملائم للنموذج الخطي وغير الخطي على الروبوت المذكور أعلاه من خلال محاولة تقديم تصميم أفضل للعناية بحدود المعالجات المتوازية ، ومشاكل مساحة العمل الصغيرة ومشاكل حركة الروبوت. في هذه الدراسة ، تم استخدام Arduino Mega لنظام التحكم. وشملت المواد الأخرى محركات السائر ثنائية القطب nema17 ومحرك مؤازر MG996R وسائق A4988 وعجلة مسننة وسلسلة وحزام وبكرة وعجلات عربات التي تجرها الدواب ، بينما تم استخدام SolidWorks لتصميم النظام والمحاكاة. تم استخدام الألومنيوم (سبيكة 6061) لبناء الروبوت نظراً لخصائصه الممتازة ومدى ملاءمته. تم تحليل المحركات والأجزاء ونمذجتها لاكتساب المعرفة بالسلوك الحركي ، وأثبتت التحليلات التحديد الخطي وغير الخطي لملاءمة النموذج. استخدمت هذه الدراسة نظاماً ملائماً للنموذج المضغوط وإجراء تحديد التحقق من الصحة بطريقتين. تظهر النتائج أنه يمكن تحديد نموذج النظام والتحقق من صحته بنجاح من البيانات المقاسة وتقديم تقدير شبه دقيق بين البيانات الافتراضية والبيانات المقاسة. أعطت عمليتا تحقق تجريبتان 94٪ باستخدام الإعداد الأول و 97٪ باستخدام الإعداد الثاني. يوفر هذا زيادة تقدم بنسبة 0.8 ٪ من الدراسات السابقة.

1. Introduction

In this century, the development and success of a country are highly dependent on its technological level and that its industries are using for construction. Robots are the top building equipment, and robotic arms have become widely used and economical in manufacturing, medicine and other industries [1]. Specifically, contour crafting (similar to 3D printing) is applied in construction, but its principle is unlike bricklaying; rather, it's like choking of mortar [2]. The manual bricklaying process has been linked with significant health hazards or problems due to the use of human labour and the slow rate of construction activities [3]. Furthermore, Semi-Automated Mason (SAM) bricklayer is also applied, but being a serial robot, it has the following demerits; less payload, less accuracy and less dynamic performance [4]. Generally, gantry robots used for bricklaying applications in construction are usually mounted and fixed in one place and equipped with parallel manipulators with small workspaces [5].

Parallel manipulators are seen as a new kind of robot other than serial manipulator [6]; it has the following merits: higher stiffness, strong bearing capacity, a small error, high precision, small weight-load ratio, very good dynamic performance, easy-to-control, etc. [7]. However, parallel manipulators have small workspace areas compared to serial manipulators. The serial manipulator has a larger workspace area, is less rigid, has a large weight-load ratio and is slower than the parallel manipulator [8]. To put this into context, the construction industry heavily relies on technological advancements and robots, particularly robotic arms. However, traditional bricklaying processes involving manual labour are associated with health hazards, slow construction rates, and limited efficiency. This study aims to address the limitations of existing gantry robots by proposing the development and performance evaluation of a novel bricklaying gantry-based parallel robot manipulator that offers enhanced flexibility, mobility, and dexterity. Specifically, the research objective includes designing a gantry-based parallel robot manipulator through the simulation of the system and the implementation of its control algorithm and evaluating the performance of the proposed robot manipulator in terms of speed, accuracy, and payload capacity to determine its effectiveness in replacing manual labour and enhancing construction rates.

The goal of this study was built on the literature review to consider some of the limitations of gantry robots, particularly regarding the lack of mobility and adequate workspace and the need to compare to footprint and the utilization of manual labour. Reviewing previous studies on robot manipulators included the study of Afolayan *et al.* [9], who developed a biomorphic carbon-filled natural rubber hyper-redundant joint mechanism robot. The researcher modelled a fish of *teleost* species (a 394.1cm Mackerel) using the biomorphic hyper-redundant joint developed. The study's control algorithm uses built-in motion patterns, and the path planning algorithm is sensor-based, and both were hosted within a single PIC18F4520 microcontroller. Furthermore, three Futaba 3003 servo motors were used to drive the joints under the control of the microcontroller control algorithm.

Karam *et al.* [10] also presented a study on the design, implementation and automation of a multi-robotic processing station. Two robot manipulators, serial and parallel robot manipulators of multi-degree of freedom, were presented. The design was to develop and test an integrated PRM and SRM system for capping plastic bottles in a scale processing line. Panda *et al.* [11] developed a gantry material handling robot for use in the bottling industry in food plants.

The design was to replace manual labour with an automated system to increase these plants' accuracy, safety and production rate. The design was also analyzed from various angles like material selection, cost and simplest and best selection of configuration. Also, Gunnar [12] developed the dynamical analysis and system identification of a Gantry-Tau parallel robot manipulator. The design was to determine the maximum stiffness of the Gantry robot manipulator. The study intended to determine the maximum in the z-direction, accomplished at the end of the research.

Also, Toby [13] proposed a robotic gantry with an end-effector for product lifting. The researcher developed a method that permits the selection of varying portions of a stack of products with the end-effector and protects the selected portions of products using a movable floor. Ye *et al.* [14] developed a variable-scale modular 3D printing robot for building interior walls. The design was to improve the efficiency of construction. The modular robot consisted of a mobile lifting module and a beam printing module. The robot can fully print complex curved interior walls under different working conditions.

From the literature review, it was observed that gantry robots are mostly mounted fixed at a place. Also, parallel manipulators have a common small workspace to footprint problem, which has got great attention and needs to be taken care of. However, this work thus considers a solution to the gap of mobility and workspace regarding current parallel manipulator designs and manual labour replacement by introducing a different gantry design with greater flexibility, mobility and dexterity. Furthermore, this study is a modification to previous studies by Gunnar [12], who considered dynamical analysis and system identification of a gantry-tau parallel manipulator, and the study of Panda *et al.* [11], who considered a gantry material handling robot for use in the bottling industry.

2. MATERIALS AND METHODS

2.1 Operation Principle of the Gantry Robot

The robot's structure, as seen in Figure 1, is a four-frame/stands figured device with dimensions of 550 x 450 x 300 mm. Each leg of the mobile robot platform is considered a serial kinematic chain (KC) made of four-link joints. The y-axis mobile platform is linked to the body frame through a sliding rail situated under; the mobile platform is driven to and fro along the y-axis by a stepper motor fixed/mounted under at both sides of the y-axis. The x-axis mobile platform is directly linked to the y-axis with the help of 2 rails situated at the 2 opposite sides of the y-axis; the platform slides horizontally along the 2 rails horizontally. The gripper is connected to the x-axis mobile platform and manipulated via the manipulator guide's aid. The end-effector guide ascends and descends along the x-axis mobile platform through the help of a toothed sprocket and chain drive.

The chain drive is driven by a toothed sprocket, driven by a stepper motor drive at the 2 adjacent sides of the x-axis mobile platform. The whole structure is movable by four 85 mm-long wheels located at the lower end of the four legs.

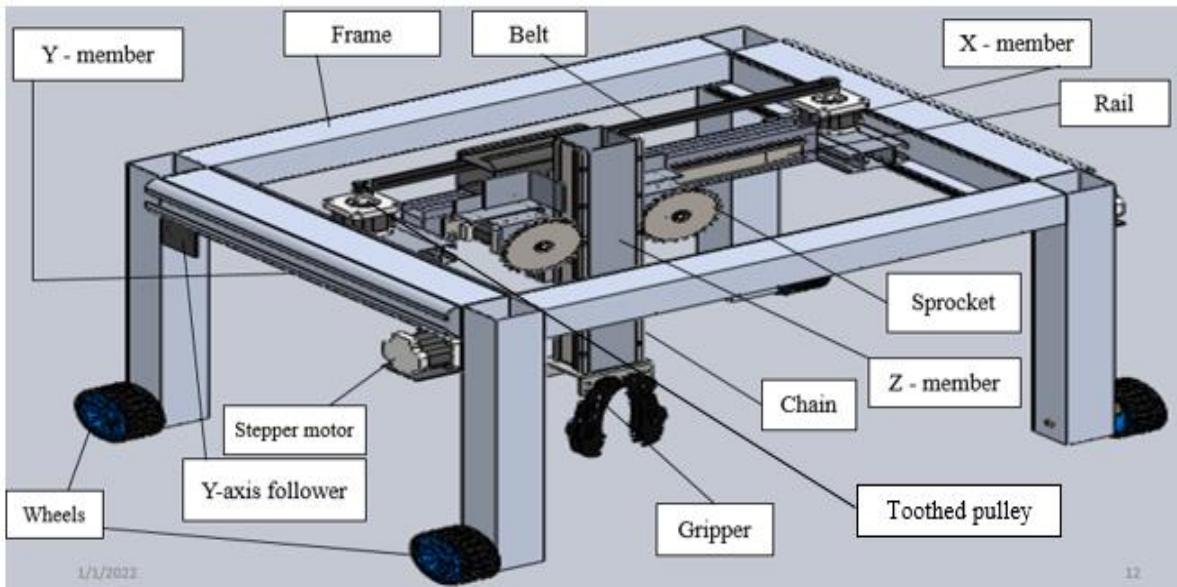


Figure 1: Gantry-based parallel robot manipulator (isometric view)

The operational user guide is shown in Figure 2 as a flowchart. It consists of switching on the device, feeding design data, defining the pick/drop spot, and going to the next working area when the current design segment is done.

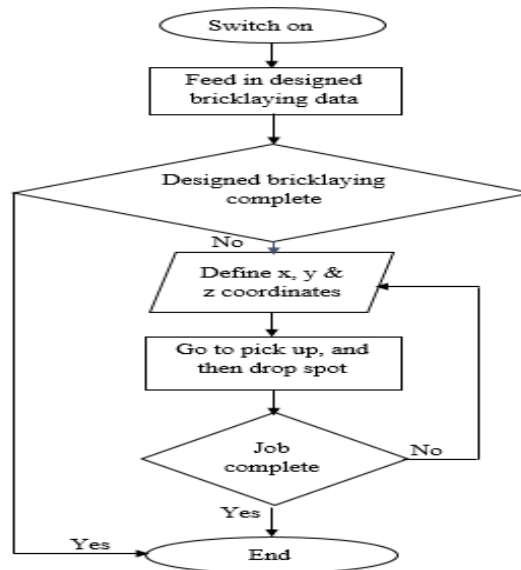


Figure 2: Flow chart showing the principle of operation of the Gantry robot

2.2 Design Consideration

The design considerations are: the robot is expected to lift a block of max. load of 100 g, a simplified control system of the joints, simplified and functional design of the joint, capturing the prototype design/geometry, material selection (e.g., speed range and power output of motor), due to cost, space and other related factors, the design is going to be a prototype, thus, a suitable multiplication scale factor must be included for enlargement to model type. Other design considerations are structure, workspace, singularities and link inference.

2.3 Material Selection

Some factors that must be considered in material selections include availability, strength, weight, ease of manufacture, damping property, etc. for stability, and system equilibrium should be observed; forces and moments should be counterbalanced [15]. Factors to consider regarding links material are strength and weight ratio since they add weight to the manipulator's actuators. Furthermore, heavy materials should be avoided as they are associated with a reduction of payload capacity. According to Meena *et al.* [16], aluminium alloy (Al 6061) is one of the materials that qualify for use because of its associated mechanical properties and hence qualify for use. Table 1 gives the properties of Al 6061.

Table 1: Mechanical and physical properties of Al 6061

Properties	Value
Density	2.70 g/cm ³
Young's Modulus	68.9 GPa
Yield Strength	276 MPa
Ultimate Tensile Strength	310 MPa
Elongation at Break	12%
Hardness (Brinell)	95 HB
Thermal Conductivity	167 W/(m·K)
Melting Point	582-652°C

2.4 Manipulator Specifications

The specifications of the parallel manipulator imply the initial design specifications and conditions imposed on it and are given in Table 2. These conditions are the dimensions, constraints, work environment, the object and weight and dimensions of work, and the required performance criteria also included.

Table 2: Specification of the objective of the design

Specification	RM Range
The magnitude of each connector/joint deflection	± 0.1 mm
The maximum magnitude of workload	1 N
Motion range magnitude in the X-direction	± 330 mm
Motion range magnitude in the Y-direction	± 360 mm
Motion range magnitude in the Z-direction	± 300 mm
Rotation angle about X, Y-axes	$\pm 90^\circ$

2.5 Manipulators Dexterity Measurement

Due to space limitations or design in manipulators, joints are constrained, and an inequality of the form is used for the measurement. $q_i^L \leq q_i \leq q_i^U$ where q_i^L is the lower limit, q_i^U is the upper limit and $i = 1, 2 \dots n$. Due to geometric constraints, there are conditions for manipulators shown in Table 3 and the workspace specification shown in Figure 3.

Table 3: Workspace boundary conditions of the RM

θ_i	Upper Limits	Lower Limits
1	0	π
2	2π	$\pi/2$

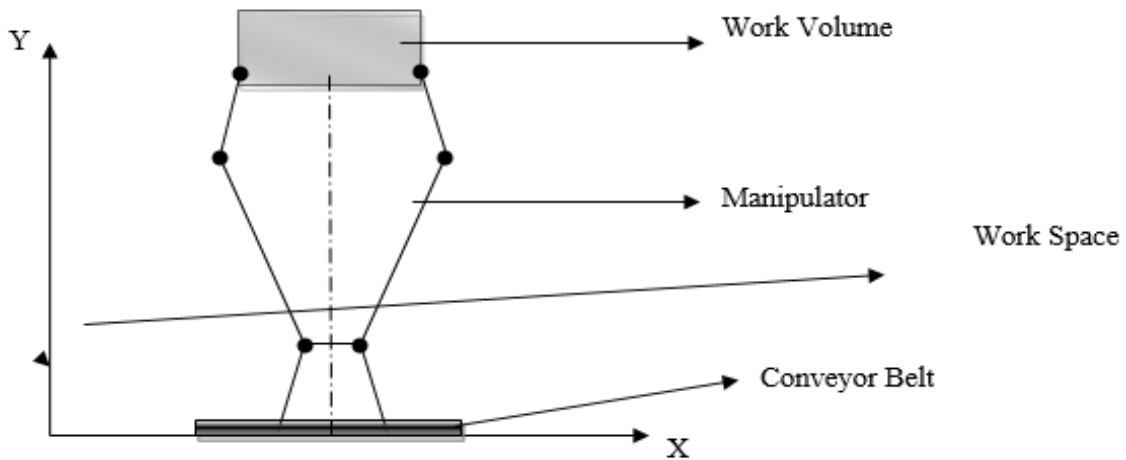


Figure 2: RM Workspace specification

2.6 Kinematic Synthesis

Typical manipulator operates in 3-D planes; this mostly requires 6-DOF. Therefore, the length of the links and actuators must be determined based on the needed workspace area and trajectory. Table 4 shows the reference.

Table 4: Specification of the length of links

Link Numbers	Lengths of Links (mm)
1	330
2	360
3	360
4	300

2.7 Robot Manipulator Mobility Analysis

The number of DOF of a robot is the number of independent parameters that must be specified for determining the position of the link relative to the body frame [17]. According to Grubler's criterion and Euler's equation, the DOF of a structure or mechanism/device can be obtained from Equations (1) and (2) [18].

$$m = \lambda(n - j - 1) + \sum_{i=1}^j f_i \quad (1)$$

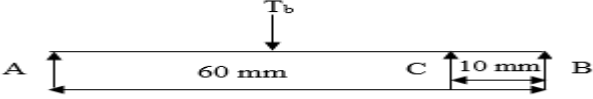
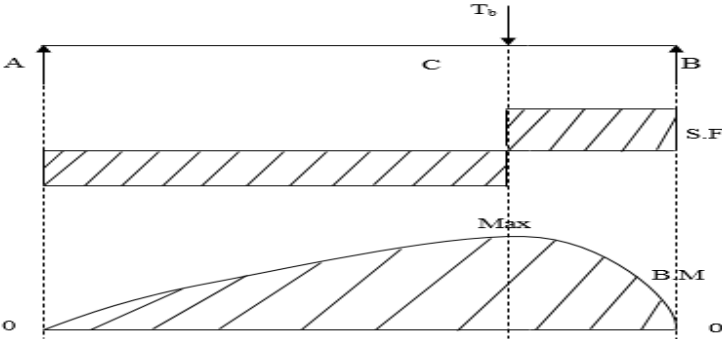
$$L = j - n + 1 \quad (2)$$

For the considered parallel manipulator, $\lambda = 6$, $n = 14$, $j = 15$ and $f_i = 15$, therefore, $m=3$ (i.e. for motion along x, y & z coordinates).

2.8 Design of the Manipulator Mechanically

The method to be adopted for the design is that the components will be designed individually and separately, that is, the modular design method. According to Hoover *et al.* [19], a dynamic model is a significant tool for the mechanical design of a structure, the ability to choose actuators, control system determination and simulation of the motion of the parallel robot manipulator. The kinematics formulations form the general basis for deriving the manipulator's dynamics. Table 5 shows the design calculation of the robot.

Table 5: Design Calculation

Initial Data	Design Calculation	Remark
<p>Maximum length sideways movement = 180 mm Length = 450 mm</p>	<p>Design for y-axis rotating shaft (y-axis follower) The maximum bending moment on the shaft</p>  <p>Shaft analysis diagram Since the pulley on the stepper motor \equiv pulley on the shaft;</p> $N_{sm} = \frac{V_{platform} \times 60}{\pi d_{pulley}}$ $N_{sm} = N_{yrr}$ $V_{pf} = \frac{180mm}{3s} = \frac{60mm}{s} = 0.06m/s$ $\theta = (180 - 2\alpha) \frac{\alpha}{180}$ $\alpha = \sin^{-1} \left[\frac{r_{p1} - r_{p2}}{x} \right] = 0$ <p>Taking $\theta = \pi rad$, $\mu = 0.25$, $K_m = 2.5$, and $K_t = 2.25$</p> <p>Shear force and bending moment diagram Obtaining shear force as well as bending moment for the shaft section, we have;</p>  $S_c = R_B - T_B = 58.02N$ $S_A = R_A, S_B = R_B$ $M_C = R_B \times 0.01 = 290.11 \times 0.01 = 2.9 Nm \Rightarrow M_{max}$ $d_{yr,r} = \sqrt[3]{\frac{16}{\pi(56 \times 10^6)} \sqrt{(2.5 \times 2.9)^2 + (2.25 \times 0.974)^2}}$	<p>$r_{p1} = r_{p2}$</p> <p>According to the ASME shaft design code, $d_{yr,r} = 8mm$</p>

<p>Consider nema 17, Sprocket standard pitch dia. = 55mm Assuming $\eta = 95\%$ $h = 300\text{mm}$ Assume 2 steppers</p>	<p>Effective Torque Required $T_{hs} = 0.36Nm$ $\eta = 95\%$ $T_{hs} = 0.36 \times 0.95$ The maximum mass of the prototype block $\Rightarrow \sum T_{hs} = (m + m_{bl})gh$ $\Rightarrow 2(0.342) = (1 + m_{bl}) \times 9.81 \times 0.3$ Force required to hold & retain the grip \RightarrowForce necessary would be thus: Assuming the efficiency of the arm is 25% $\Rightarrow \sum T_s = 0.25 \times 1.08 = 0.27Nm$ Hence $m_{bl} = \frac{\sum T_s}{gh} = \frac{0.27}{9.81 \times 0.3} \cong 0.09kg$</p>	<p>$T_{hs} = 0.342Nm$ $m_{bl} = 0.77kg$ $\sum T_s = 0.27Nm$ $m_{bl} = 0.09kg$</p>
<p>Density of MDF wood = 800kg/m^3 $v_{bl} = l_{bl} \times b_{bl} \times h_{bl}$</p>	<p>Length of Block (modelled) $m_{bl} = \rho_{bl} \times v_{bl}$ $0.09 = 800 \times v_{bl} \times 0.035 \times 0.016 \Rightarrow v_{bl} = 0.234\text{mm}$ $\Rightarrow v_{bl} \cong 200.89\text{mm}$ For the convenience of the grip, this length is divided in 3 \Rightarrow size for the downscale $\Rightarrow 65\text{mm} \times 35\text{mm} \times 16\text{mm}$</p>	<p>$v_{bl} = 200.89\text{mm}$</p>
<p>$p = \text{pitch} = 6\text{mm}$ (chain) $z = \text{no of teeth} = 28$</p>	<p>The speed required for the stepper motor $v = \frac{pzn}{1000} \Rightarrow N = \frac{v \times 1000}{p \times z} = \frac{6 \times 1000}{6 \times 28}$ $\Rightarrow N \cong 35.71\text{rpm} \Rightarrow N = 40\text{rpm}$</p>	<p>$N = 40\text{rpm}$</p>
<p>mass = density \times volume $m_z = 2.5\text{kg}$ $h_z = 0.3\text{mm}$</p>	<p>Z-axis required torque $\Rightarrow \sum m_z = 0.15 \times 2.5 = 0.375\text{kg}$ $T_z = \sum m_z \times g \times h_z = 0.375 \times 9.81 \times 0.3$ $T_z = 110Nm$</p>	<p>$T_z = 110Nm$</p>
<p>The Z-component also added 0.375kg to the mass. Hence, 2 steppers motor would be sufficient</p>	<p>X-axis required torque Mass of x-axis members; $m_x = 0.97\text{kg}$ $\sum m_x = \mu \times m_x = 0.15 \times 0.97 = 0.15\text{kg}$ Hence torque required $\Rightarrow \sum m_x \times g \times h = 0.15 \times 9.81 \times 0.3$, $T_x = 0.44Nm$ Provided 1 motor provides 0.36Nm; hence 2 motors are required for x-axis motion. $\sum T_x = (0.36 \times 2) \times \eta_b \Rightarrow 0.36 \times 2 \times 0.95 = 0.68Nm$ $\sum T_x > T_x$, hence is sufficient.</p>	<p>$T_x = 0.68Nm$ $\sum T_x > T_x$</p>

<p>The X-component also added 0.15kg to the mass. Hence, 2 steppers motor would be sufficient</p>	<p>Y-axis required torque Mass of x-axis members; $m_y = 1.2kg$ $\sum m_y = \mu \times m_y = 0.15 \times 1.2 = 0.18kg$ Hence torque required $\Rightarrow \sum m_y \times g \times h = 0.18 \times 9.81 \times 0.36$, $T_y = 0.64Nm$ Provided 1 motor provides 0.36Nm; hence 2 motors are required for x-axis motion. $\sum T_y = (0.36 \times 2) \times \eta_b \Rightarrow 0.36 \times 2 \times 0.95 = 0.66Nm$ $\sum T_y > T_y$, hence is sufficient.</p>	<p>$T_y = 0.66Nm$ $\sum T_y > T_y$</p>
<p>Motor selection</p>	<p>(viii) Motor selection criterion From belt calc., Power req. = 7.792W Stepper motor phases = 4. Each phase draws 1.7A at 2.8V $\therefore I$ (total) = 1.7 x 4 = 6.8A, V(total) = 2.8 x 4 = 11.2V Thus, Power = I x V = 6.8 x 11.2</p>	<p>$P = 76.16W$ $= 0.07616KW$</p>
<p>Total power input, used & lost</p>	<p>(ix) Total power required & loss Stepper input & used current = 5A Stepper input & used voltage = 12V & 11.2V, respectively. Servo input & used current = 50mA Servo input & used voltage = 5V & 4.8V respectively Stp. $T_{power-input} = 5 \times 12 = 60W \times 6$ (6steppers) = 360W Belt $T_{power-input} = (7.792 \times 2) + 7.792 / 2 = 19.48W$ Servo $T_{power-input} = 5 \times 50mA = 0.25W$ $T_{power-input} = (360 + 19.48 + 0.25) W = 379.73W$</p>	<p>$T_{power-input} = 379.73W$</p>
	<p>Stp. $T_{power-used} = 5 \times 11.2 = 56W \times 6$ (6steppers) = 336W Belt $T_{power-used} = 19.48W$ Servo $T_{power-used} = 4.8 \times 50mA = 0.24W$ $T_{power-used} = (336 + 19.48 + 0.24) W = 355.72W$ $T_{power-loss} = T_{power-input} - T_{power-used} = 379.73 - 355.72$</p>	<p>$T_{power-used} = 355.72W$ $T_{power-loss} = 24.01W$</p>

2.9 Circuit Diagram Showing Motors Connection

The microcontroller used for system control was Arduino Mega. The stepper motors 1 & 2 were used for x-axis motion drive, motors 3 & 4 for y-axis motion and motors 5 & 6 for z-axis motion control. From the circuit diagram shown in Figure 4, the servo motor at the bottom of the circuit was used as the gripper for picking and dropping the bricks.

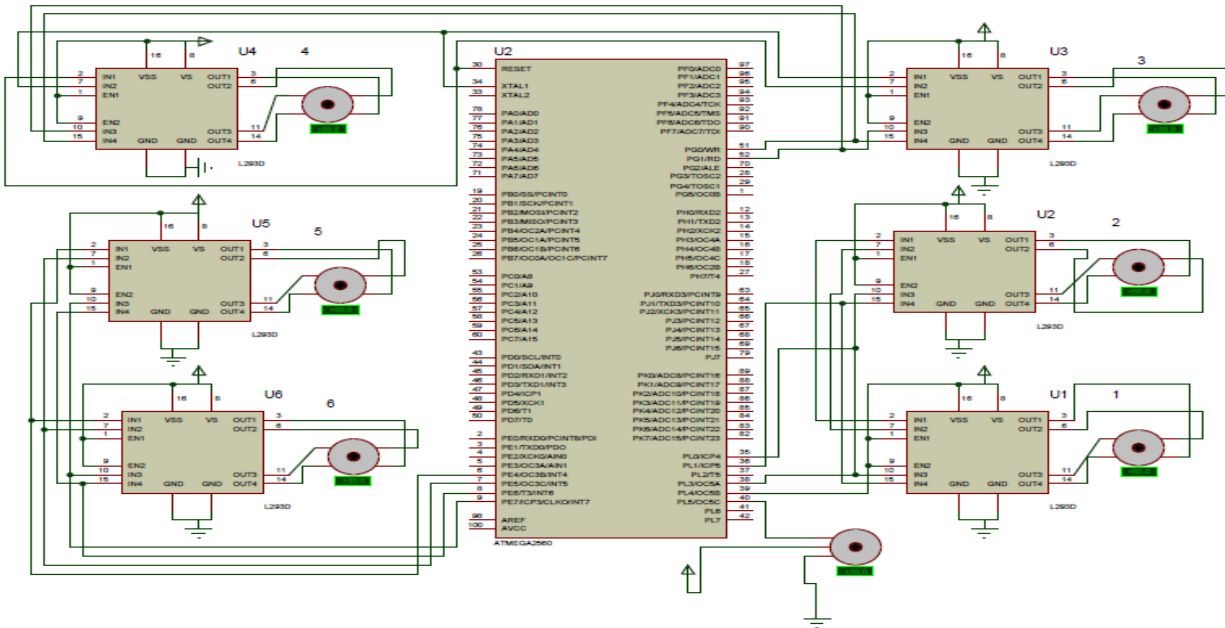


Figure 4: Circuit diagram showing motors connection

A4988 was the driver for the stepper motors, but in the proteus environment, L293D was used as a substitute. The A4988 driver requires two capacitors, 47 μ f, 50V and 100 μ f, 25V but L293D contains those capacitors embedded, so none is shown on the circuit diagram.

The power supply unit used was digital Tektronix, capable of providing the required 6A and 12V power as stated in the design calculation table (Table 5).

3. Results and discussion

3.1 Simulation Results of the Gantry Robot and Discussion

From the result obtained in Figure 5(a), (b), and (c), the constructed robot material (Al alloy) has a yield strength of 276 MPa, the Z-member maximum load produced 12.57 MPa, the X-member maximum load produced 4.814 MPa, and the robot frame maximum load produced 13.34 MPa. All the 3 members were subjected to stresses below the design yield strength of the robot material. Furthermore, for any good and acceptable design, the design yield strength should never be more than 25% of the yield strength of the material under any given condition [20]. Since the material yield strength is 276 MPa, the design yield strength is 15% of the material yield strength by conversion. Thus, the device would function effectively from a strength point of view. Thus, this result represents good and acceptable structures or members' designs mechanically.

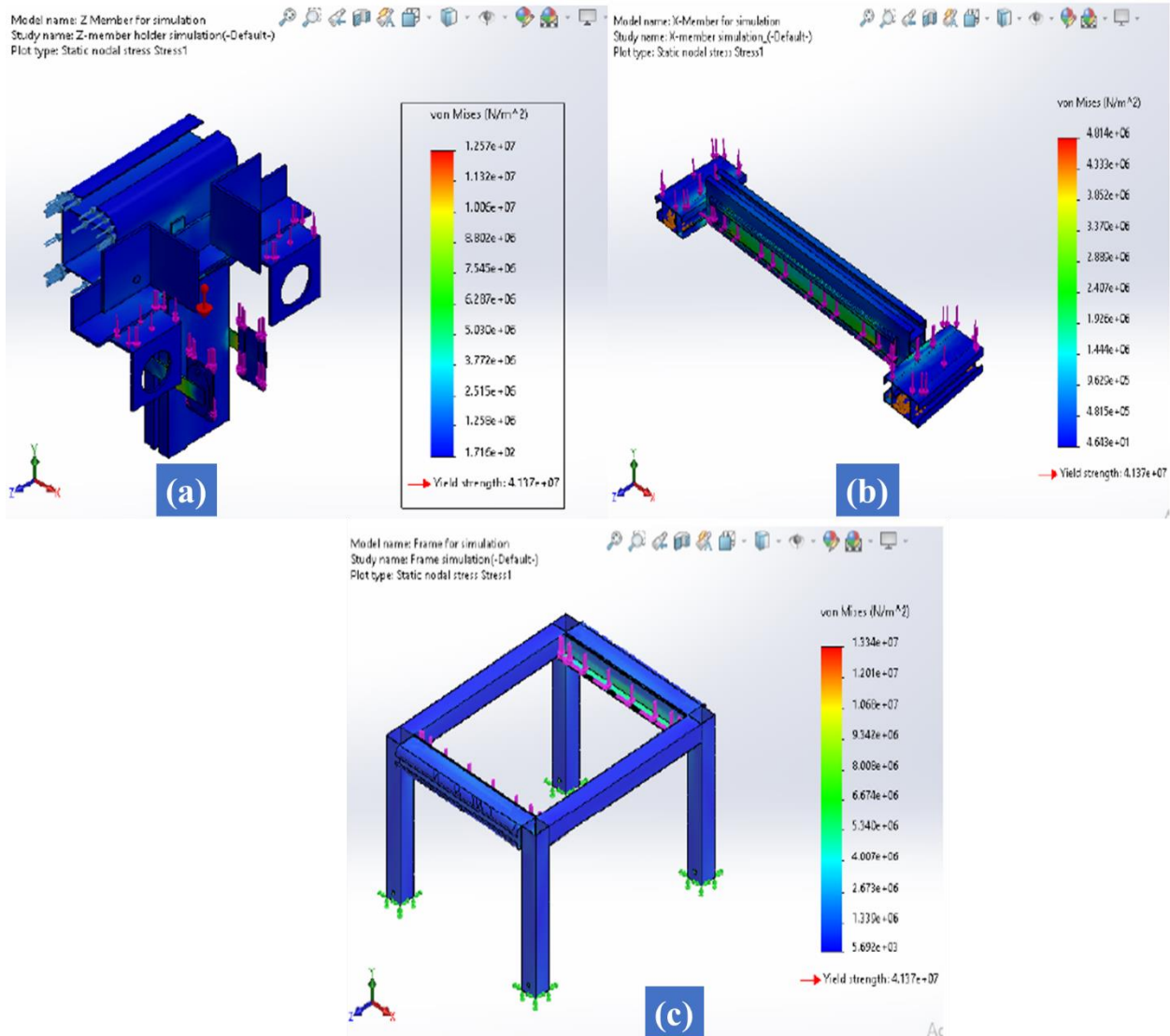


Figure 5: Stress simulation result of (a) Z-member, (b) X-member, and (c) Robot frame

3.2 Performance Efficiency Measuring Procedure of the Gantry Robot

In conducting a performance efficiency test for the device, a 2D planer map having a series of uniform rectangular boxes (i.e., x-y plane) was constructed using 2D cardboard paper, as seen in Figure 6. Hence, the gantry robot was placed on the map on the floor to such an extent that it occupied half of the planer map. These uniform rectangular boxes were the same size as the width of the scaled building blocks. Previous studies such as Zou *et al.* [21] and Sonar *et al.* [22] employed a similar approach.

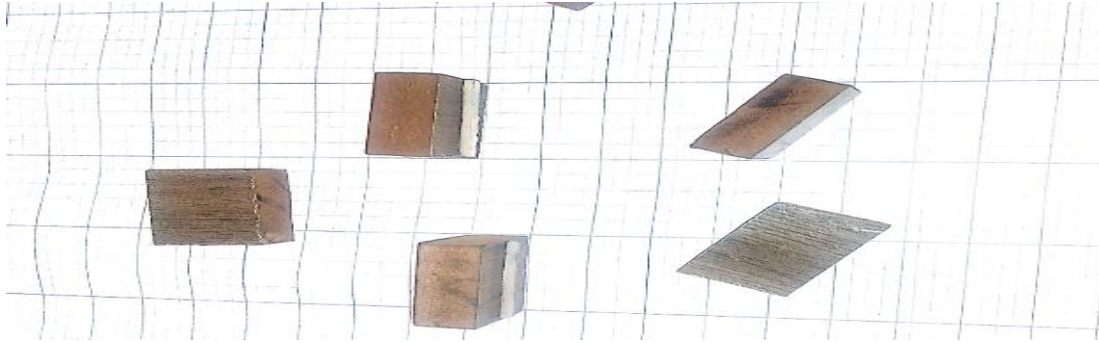


Figure 6: 2D planar map

The first approach was keeping y-values fixed on level one. Block placement graph boxes are drawn on a plain sheet titled a 2D planar map for each evaluation procedure carried out while increasing level values of x in ascending order. The boxes were numbered as follows; first box value = level 1, second box value = level 2..... nth box value = level n. Figure 7 shows the obtained result. The second approach was keeping in ascending order increasing both level values of x and y exclusively and correspondingly at a time. Figure 8 illustrates the results of the procedure. Results obtained in Figures 7 and 8 showed that the best-fit lines on the x and y axes are linear.

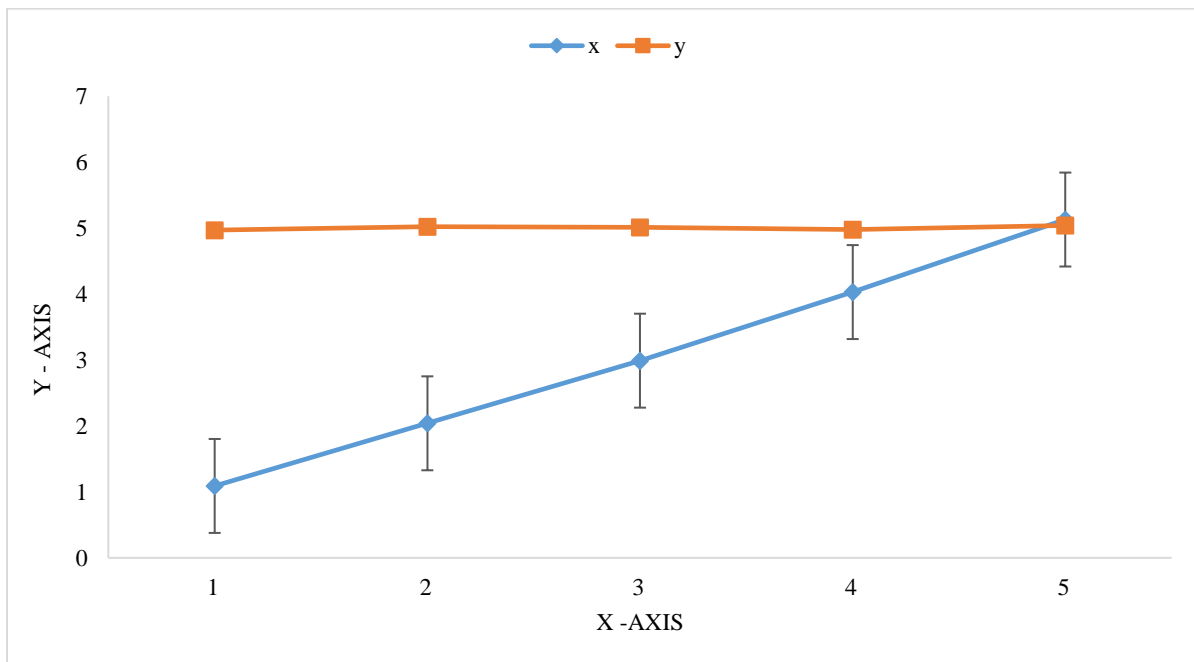


Figure 7: 1st setup of the 2D planar map of the robot under constant y-values

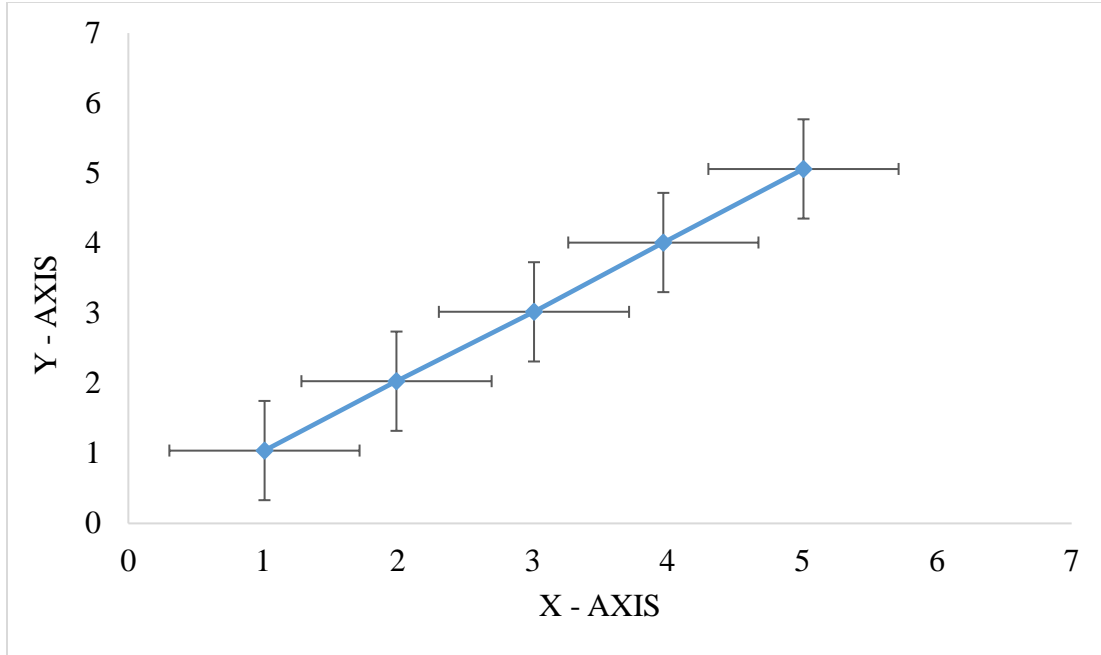


Figure 8: 2nd setup of the 2D planar map of the robot under varying x and y-values

3.3 Model Fit and Validation

Ljung [23] developed an ideology, later developed into a method called System Identification. It involves feeding a system or system joints with data (e.g., displacement, velocity, torque, etc.), then building a hypothesis by predicting the output and measuring the actual output. Hofer and D'Andrea [24] and Gale *et al.* [25] employed the same approach to improve a robotic manipulator model based on multivariate residual modelling. The validation of this model is given in Equation (3).

$$fit = 100 \left[1 - \frac{\sqrt{\sum_{t=1}^N (y(t) - \hat{y}(t))^2}}{\sqrt{\sum_{t=1}^N (y(t) - \bar{y})^2}} \right] \quad (3)$$

Where from Figure 7,

$y(t)$ = measured value = 5.13mm

$\hat{y}(t)$ = predicted value = 5mm

\bar{y} = mean value of $y(t)$ = 3.06mm

And from Figure 8,

$y(t)$ = measured value = 5.14mm

$\hat{y}(t)$ = predicted value = 5mm

\bar{y} = mean value of $y(t)$ = 3.08mm

Hence, from Equation (3), for the 1st setup, fit =94%; for the 2nd setup, fit=97%. From the results obtained, it can be justified that the model is well-fitted with values of 94% and 97% from the first and second approaches, respectively. It is important to note that these approximately 3-6% fitting errors can be attributed to several factors, including measurement inaccuracies, inherent system noise, and modelling assumptions. The slight deviations between the predicted and measured values are within an acceptable range considering the complexity of the system and the inherent uncertainties involved. These results were obtained from the average of the methodology repetition as a means of cross-evaluation. Comparing this result (with an average model fit of 95.5%) with that of the cross-validation of the study by Gunnar [12], an average model fit of 95.16%, it can be observed that the developed model shows promising results of manipulator mobility; hence, it can be said to be logically and technically justified as it falls within the expected and acceptable range of literature.

4. Conclusions

In this study, a novel gantry-based parallel robot manipulator was developed and evaluated for bricklaying applications in the construction industry. The objective was to design and simulate the robot manipulator, implement a control algorithm, and evaluate its speed, accuracy, and payload capacity. The gantry-based parallel robot manipulator was designed and analyzed using appropriate design considerations, material selection, and kinematic synthesis. The robot's operational principle and design specifications were carefully defined, and the necessary calculations and simulations were performed to ensure the structural integrity and performance of the manipulator. Simulation results demonstrated that the robot design met the strength requirements, with stress values well below the yield strength of the chosen material. The performance efficiency of the robot was evaluated through a 2D planar map test, where different setups were assessed. The results indicated linear relationships and demonstrated the robot's ability to perform bricklaying tasks effectively.

Furthermore, the model fit and validation were carried out using a system identification approach. The developed model showed good fitting with measured values, achieving 94% and 97% fit for the first and second setups, respectively. These fitting errors of approximately 3-6% can be attributed to various factors but still fell within an acceptable range considering the complexity of the system and inherent uncertainties. The study successfully designed and evaluated a gantry-based parallel robot manipulator for bricklaying applications. The developed robot demonstrated enhanced mobility, workspace utilization, and promising speed, accuracy, and payload capacity results. The findings of this study contribute to the advancement of robotic systems in the construction industry, offering potential benefits in terms of efficiency, safety, and productivity.

ACKNOWLEDGEMENTS

The authors acknowledge the support offered by Engr. Awwal Isa Bello, Mallam Ibrahim and Mallam Musa Nari, as well as the Department of Mechanical Engineering staff and students, Ahmadu Bello University, Zaria, Nigeria.

Conflicts of Interests

The authors declare no competing interests

Authors' Contributions

M.H.I. is responsible for data collection, methodology, and writing of the original draft. U.A.U. is responsible for the conceptualization, supervision, methodology and writing of the original draft. M.A.O. is responsible for the conceptualization, supervision and methodology. A.N.O. is responsible for the data analysis and review of the original draft.

5.References

- [1] M. Javaid, A. Haleem, R. P. Singh, and R. Suman, "Substantial capabilities of robotics in enhancing industry 4.0 implementation," *Cognitive Robotics*, vol. 1, pp. 58–75, Jan. 2021, doi: 10.1016/J.COGR.2021.06.001.
- [2] S. Luhar and I. Luhar, "Additive Manufacturing in the Geopolymer Construction Technology: A Review," *The Open Construction & Building Technology Journal*, vol. 14, no. 1, pp. 150–161, Aug. 2020, doi: 10.2174/1874836802014010150.
- [3] O. Adepoju, "Robotic Construction Technology," *Springer Tracts in Civil Engineering*, pp. 141–169, 2022, doi: 10.1007/978-3-030-85973-2_7/COVER.
- [4] T. Bruckmann, H. Mattern, A. Spengler, C. Reichert, A. Malkwitz, and M. König, "Automated Construction of Masonry Buildings using Cable-Driven Parallel Robots".
- [5] F. P. Bos *et al.*, "The realities of additively manufactured concrete structures in practice," *Cem Concr Res*, vol. 156, p. 106746, Jun. 2022, doi: 10.1016/J.CEMCONRES.2022.106746.
- [6] C. Y. Lai, D. E. Villacis Chavez, and S. Ding, "Transformable parallel-serial manipulator for robotic machining," *International Journal of Advanced Manufacturing Technology*, vol. 97, no. 5–8, pp. 2987–2996, Jul. 2018, doi: 10.1007/S00170-018-2170-Z/METRICS.
- [7] C. Yang, W. Ye, and Q. Li, "Review of the performance optimization of parallel manipulators," *Mech Mach Theory*, vol. 170, p. 104725, Apr. 2022, doi: 10.1016/j.mechmachtheory.2022.104725.
- [8] R. Simoni, P. R. Rodriguez, P. Cieslak, L. Weihmann, and A. P. Carboni, "Design and kinematic analysis of a 6-DOF foldable/deployable Delta parallel manipulator with spherical wrist for an I-AUV," *OCEANS 2019 - Marseille, OCEANS Marseille 2019*, vol. 2019-June, Jun. 2019, doi: 10.1109/OCEANSE.2019.8867496.

- [9] M. O. Afolayan, D. S. Yawas, C. O. Folayan, and S. Y. Aku, "Mechanical Description of a Hyper-Redundant Robot Joint Mechanism Used for a Design of a Biomimetic Robotic Fish," *Journal of Robotics*, vol. 2012, pp. 1–16, 2012, doi: 10.1155/2012/826364.
- [10] Z. A. Karam and M. A. Neamah, "Design, Implementation, Interfacing and Control of Internet of Robot Things for Assisting Robot," *International Journal of Computing and Digital Systems*, vol. 11, no. 1, pp. 387–399, 2022, doi: 10.12785/IJCDS/110132.
- [11] B. K. Panda, S. S. Panigrahi, G. Mishra, and V. Kumar, "Robotics for general material handling machines in food plants," *Transporting Operations of Food Materials within Food Factories: Unit Operations and Processing Equipment in the Food Industry*, pp. 341–372, Jan. 2023, doi: 10.1016/B978-0-12-818585-8.00005-2.
- [12] J. Gunnar, "Dynamical Analysis and System Identification of the Gantry-Tau Parallel Manipulator," 2005, Accessed: May 13, 2023. [Online]. Available: <https://urn.kb.se/resolve?urn=urn:nbn:se:liu:diva-5322>
- [13] "Robotic gantry with end effector for product lifting," Nov. 2018.
- [14] C. Ye, N. Chen, L. Chen, and C. Jiang, "A variable-scale modular 3D printing robot of building interior wall," *Proceedings of 2018 IEEE International Conference on Mechatronics and Automation, ICMA 2018*, pp. 1818–1822, Oct. 2018, doi: 10.1109/ICMA.2018.8484433.
- [15] A. N. Oyediji, U. A. Umar, L. S. Kuburi, A. A. Edet, and Y. Mukhtar, "Development and performance evaluation of an oil palm harvesting robot for the elimination of ergonomic risks associated with oil palm harvesting," *Journal of Agricultural Engineering*, vol. 53, no. 3, Sep. 2022, doi: 10.4081/JAE.2022.1388.
- [16] J. Meena, T. K. Sunil Kumar, and T. R. Amal, "Design and Implementation of a Multi-purpose End-effector Tool for Industrial Robot," *2021 International Symposium of Asian Control Association on Intelligent Robotics and Industrial Automation, IRIA 2021*, pp. 70–76, Sep. 2021, doi: 10.1109/IRIA53009.2021.9588746.
- [17] K. Mohamed, H. Elgamal, and A. Elsharkawy, "Dynamic analysis with optimum trajectory planning of multiple degree-of-freedom surgical micro-robot," *Alexandria Engineering Journal*, vol. 57, no. 4, pp. 4103–4112, Dec. 2018, doi: 10.1016/J.AEJ.2018.10.011.
- [18] E. V. Gaponenko, D. I. Malyshev, and L. Behera, "Approximation of the parallel robot working area using the method of nonuniform covering," *J Phys Conf Ser*, vol. 1333, no. 5, p. 052005, Oct. 2019, doi: 10.1088/1742-6596/1333/5/052005.
- [19] A. M. Hoover, E. Steltz, and R. S. Fearing, "RoACH: An autonomous 2.4g crawling hexapod robot," *2008 IEEE/RSJ International Conference on Intelligent Robots and Systems, IROS*, pp. 26–33, 2008, doi: 10.1109/IROS.2008.4651149.

- [20] R. V. Martinez *et al.*, “Robotic Tentacles with Three-Dimensional Mobility Based on Flexible Elastomers,” *Advanced Materials*, vol. 25, no. 2, pp. 205–212, Jan. 2013, doi: 10.1002/ADMA.201203002.
- [21] Z. Zou *et al.*, “Real-time Full-stack Traffic Scene Perception for Autonomous Driving with Roadside Cameras,” *Proc IEEE Int Conf Robot Autom*, pp. 890–896, 2022, doi: 10.1109/ICRA46639.2022.9812137.
- [22] H. A. Sonar, J.-L. Huang, and J. Paik, “Soft Touch using Soft Pneumatic Actuator–Skin as a Wearable Haptic Feedback Device,” *Advanced Intelligent Systems*, vol. 3, no. 3, p. 2000168, Mar. 2021, doi: 10.1002/AISY.202000168.
- [23] L. Ljung, “System Identification,” pp. 163–173, 1998, doi: 10.1007/978-1-4612-1768-8_11.
- [24] M. Hofer and R. D’Andrea, “Design, Modeling and Control of a Soft Robotic Arm,” *IEEE International Conference on Intelligent Robots and Systems*, pp. 1456–1463, Dec. 2018, doi: 10.1109/IROS.2018.8594221.
- [25] S. Gale, H. Rahmati, J. T. Gravdahl, and H. Martens, “Improvement of a Robotic Manipulator Model Based on Multivariate Residual Modeling,” *Front Robot AI*, vol. 4, p. 28, Jul. 2017, doi: 10.3389/FROBT.2017.00028/BIBTEX.